Pressure effect on luminescence dynamics in Pr³⁺-doped LiNbO₃ and LiTaO₃ crystals

W Gryk[1], C Dujardin[2], M-F Joubert[2], W Ryba–Romanowski[3], M Malinowski[4] and M Grinberg[1]

[1] Institute of Experimental Physics, University of Gdańsk, Wita Stwosza 57, 80-952 Gdańsk, Poland
[2] LPCML, UMR 5620 CNRS, Université Claude Bernard Lyon 1, Domaine Scientifique de la Doua, 10 rue Ampère, 69622 Villeurbanne cedex, France
[3] Institute of Low Temperature and Structural Research, Polish Academy of Science, Wrocław, Poland
[4] Institute of Microelectronics and Optoelectronics, Warsaw Technical University, Koszykowa 75, 00-662 Warsaw, Poland

Abstract
The $^1D_2 \rightarrow \ ^3H_4$ luminescence kinetics of LiNbO₃:Pr³⁺ and LiTaO₃:Pr³⁺ have been measured under high hydrostatic pressure applied in a diamond anvil cell for pressures up to 200 kbar. The luminescence decays have been analysed using the continuous function decay times distribution. Two mechanisms that accelerate the emission decays with increasing pressure have been proposed: the non-radiative depopulation of the $^1D_2$ state through the Pr³⁺ trapped exciton, dominating in LiNbO₃:Pr³⁺ and pressure-induced increase of the $^1D_2 \rightarrow \ ^3H_4$ transition probability, dominating in LiTaO₃:Pr³⁺.

1. Introduction

The interest in crystals of LiXO₃ (X = Nb, Ta) type doped with transition-metal and rare-earth ions results from the fact that they offer simultaneously electro-optics, nonlinear effects [1, 2] and lasing ability. Interest in the doping of the laser materials with praseodymium has been renewed owing to the broad spectral range of Pr³⁺ emission that extends from the UV to IR [3].

The spectral properties of LiNbO₃ doped with Pr³⁺ have been investigated by several authors [4–7] and detailed analysis of the energetic structure of the 4f² electronic configuration of the Pr³⁺ ion has been done by Muñoz-Santiuste *et al* [6]. There are much fewer works on the spectroscopy of LiTaO₃:Pr³⁺ [8, 9]. The energetic structure of the lowest states of the Pr³⁺ (4f²) system is presented in figure 1. The ground state is the $^3H_4$ multiplet, that is split by the crystal field of C₃ᵥ symmetry into three doubly degenerate Γ_3 states, and three non-degenerate states (two Γ_1 and one Γ_2). The most efficiently emitting excited states are $^1D_2$ split into $\Gamma_1\Gamma_3$, and $^3P_0$, that C₃ᵥ symmetry transforms as the irreducible representation Γ_1.
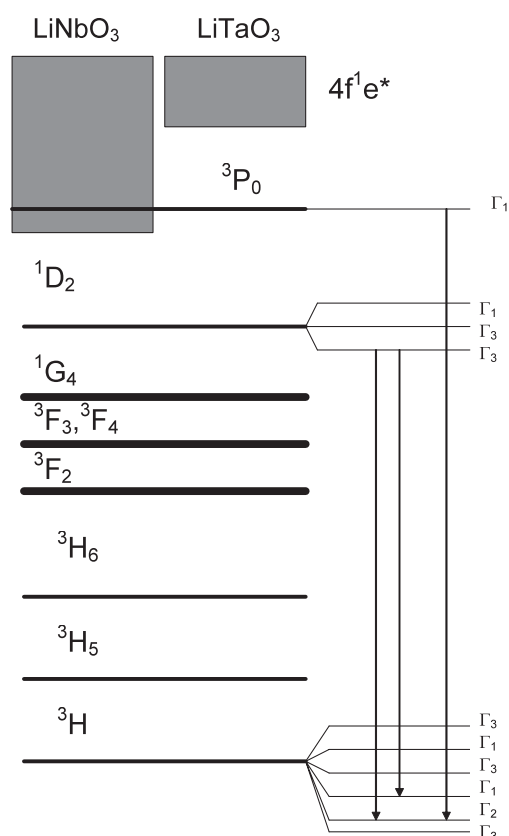
Figure 1. Energetic structure of the lowest states of the Pr^{3+} ion system in $LiNbO_3$ and $LiTaO_3$ crystals. The $4f^2$ electronic configuration states are indicated by respective lines (with the same energy in both materials). The positions of the lowest state of the Pr^{3+} trapped exciton $4f^1e*$ are indicated as the respective grey bands.

The dominating emissions related to the $^3P_0 \rightarrow\ ^3H_4$ and $^1D_2 \rightarrow\ ^3H_4$ transitions represent in fact the $\Gamma_1(^1D_2) \rightarrow \Gamma_2, \Gamma_3(^3H_4)$ and $\Gamma_3(^1D_2) \rightarrow \Gamma_2\Gamma_3(^3H_4)$ and $\Gamma_3(^1D_2) \rightarrow \Gamma_1(^3H_4)$ transitions, respectively [9].

Although the crystal and electronic structures of $LiNbO_3$ and $LiTaO_3$ are similar, the optical properties of Pr^{3+} in $LiNbO_3$ and $LiTaO_3$ are different. The absorption edge of $LiNbO_3:Pr^{3+}$ appears for an energy about 2000 cm^{-1} lower than that of $LiTaO_3:Pr^{3+}$. In both cases the Pr^{3+} luminescence excitation spectrum has been found to have structure over the absorption edge [9, 10]. This structure was attributed to the localized states, broadened by electron–phonon interaction, related to the exciton trapped at the Pr^{3+} ion. It has been considered that the exciton is created by a hole at a Pr ion (Pr^{4+}) and an electron partly delocalized in the lattice attracted by the Coulomb potential of the hole [9]. In figure 1 these states are presented by the grey bands. As a result of the lower energy of the trapped exciton, it influences the f–f transitions much more strongly in the case of $LiNbO_3:Pr^{3+}$. The most spectacular effect is that the efficiency of the luminescence related to the $^3P_0 \rightarrow\ ^3H_4$ transition is much weaker in $LiNbO_3:Pr^{3+}$ than in $LiTaO_3:Pr^{3+}$.

In both materials the Pr^{3+} ions occupy the octahedrally coordinated Li^+ sites (this has been demonstrated for $LiNbO_3:Pr^{3+}$ by Rutherford backscattering spectroscopy [11]). Since such

a position of Pr^{3+} needs charge compensation, multisite effects in both $LiNbO_3$ and $LiTaO_3$ are expected. For instance, the structure of the absorption corresponding to the $^3H_4 \rightarrow {}^3P_0$ transition in Pr^{3+} in $LiNbO_3$ was related to the existence of four different Pr^{3+} sites [6, 12].

We have used high hydrostatic pressure to tune the crystal field strength and have investigated the luminescence spectra related to the $^3P_0 \rightarrow {}^3H_4$ and $^1D_2 \rightarrow {}^3H_4$ transitions in $LiNbO_3{:}Pr^{3+}$ [10, 13] and $LiTaO_3{:}Pr^{3+}$ [9]. We have found that in both materials the energy of the lowest state of trapped exciton diminishes with pressure, and this effect results in quenching of the emission related to the $^1D_2 \rightarrow {}^3H_4$ transition in Pr^{3+} in $LiNbO_3{:}Pr^{3+}$ and emission related to the $^3P_0 \rightarrow {}^3H_4$ transition in $LiTaO_3{:}Pr^{3+}$.

In this paper we present the $^1D_2 \rightarrow {}^3H_4$ luminescence kinetics measurements of the $LiNbO_3{:}Pr^{3+}$ and $LiTaO_3{:}Pr^{3+}$ for the pressure range up to 200 kbar. Our results confirm the existence of the localized states related exciton trapped at Pr^{3+} and allowed to analyse the influence of these states on the efficiency and kinetics of the Pr^{3+} ion emission related to the $^1D_2 \rightarrow {}^3H_4$ transition.

2. Experiments

2.1. Luminescence and luminescence decay measurements

The $LiNbO_3{:}Pr^{3+}$ crystals were obtained by Czochralski method at the I.T.M.E. Laboratory in Warsaw. $LiNbO_3$ samples with concentrations of 0.1, 0.5 and 1 at.% of Pr^{3+} ions were grown from a congruent melt (Li/Nb = 0.94) parallel to the $\langle c \rangle$ direction. Details of the growth process are described in [14]. The data presented in this paper were obtained for $LiNbO_3{:}Pr^{3+}$ with 0.5 at.% of Pr^{3+}.

The $LiTaO_3{:}Pr^{3+}$ crystal was grown from a congruent melt (Li/Ta = 0.94) by the Czochralski method. The concentration of Pr^{3+} ions, estimated by chemical analysis, was 0.4 at.%. Details of the crystal growth are described in [8, 15].

Pressure was applied in a diamond anvil cell (DAC) type D04 designed and produced by Diacell Product Inc. Poly (dimethylsiloxane) oil was used as the pressure-transmitting medium, and a small piece of ruby crystal was used as the pressure detector.

Luminescence kinetics were measured under excitation at 10 Hz by a dye laser (courmarin 460) pumped at 308 nm by an eximer laser (Lumonics). The pulse duration was around 10 ns. The signal was collected by a cooled AsGa PMT through a monochromator and was analysed by a multichannel analyser (Canberra). The time per channel was adjusted to the decay. Due to the parasitic effect the first 100 ns of each decay are not reliable, and were not considered.

In both cases, $LiNbO_3$ and $LiTaO_3$, emission was monitored at 618 nm, which corresponds to the $^1D_2 \rightarrow {}^3H_4$ transition of the Pr^{3+} ion. The monitored wavelength was changed with increasing pressure due to the existence of red pressure shift of the $^1D_2 \rightarrow {}^3H_4$ emission. Selected emission spectra for $LiNbO_3{:}Pr^{3+}$ and $LiTaO_3{:}Pr^{3+}$ are presented in figures 2(a) and (b).

Decay curves obtained for the $LiNbO_3{:}Pr^{3+}$ and $LiTaO_3{:}Pr^{3+}$ are presented in figure 3(a) and (b), respectively. One notices that all decays are not single-exponential. Also, it is evident that for both materials the emission decays faster when the pressure is increased. Additionally, we have observed the effect of damping of the $^1D_2 \rightarrow {}^3H_4$ emission of Pr^{3+} ion in $LiNbO_3{:}Pr^{3+}$, and the appearance of the broad band emission related to the recombination of trapped exciton [13]. Therefore, we were not able to measure the $^1D_2 \rightarrow {}^3H_4$ emission in $LiNbO_3{:}Pr^{3+}$ at a pressure above 100 kbar. No such effect has been observed in $LiTaO_3{:}Pr^{3+}$ up to 200 kbar.
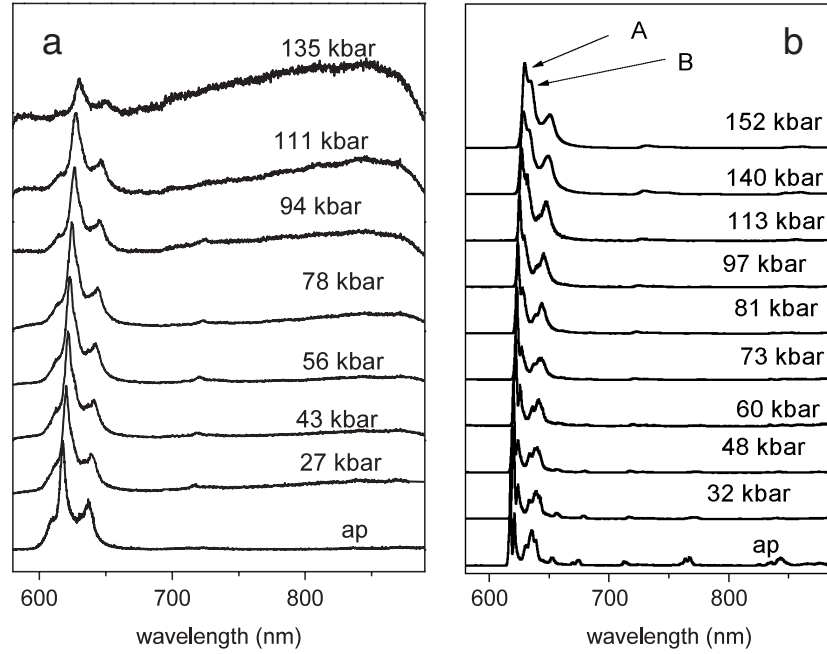
Figure 2. $^1D_2 \rightarrow {}^3H_4$ luminescence spectrum for selected pressures for LiNbO$_3$:Pr^{3+} (a) and LiTaO$_3$:Pr^{3+} (b).

2.2. Analysis of the luminescence decays

It is seen that the decays presented in figures 3(a) and (b) cannot be easily and unambiguously decomposed into a particular number of single exponential decays. This is one reason why we have decomposed the luminescence decays using a continuous function of the decay time.

We have assumed that the emission is inhomogeneous due to the multisite effect and that each individual Pr^{3+} ion luminescence contributes to the total emission through the single exponential decay labelled by the decay constant τ:

$$I_\tau(t) = \frac{A(\tau)}{\tau} e^{-t/\tau}. \tag{1}$$

One notices that in the relation (1) τ is the effective lifetime related to the radiative and non-radiative lifetimes τ_r and τ_{nr} as follows:

$$\tau^{-1} = \tau_r^{-1} + \tau_{nr}^{-1}. \tag{2}$$

In such a way relation (2) allows us to cover the situation when donor–acceptor energy transfer is responsible for 'not single-exponential' emission decays. The function

$$A(\tau) = A_0(\tau_r) \frac{\tau}{\tau_r} \tag{3}$$

and the function $A_0(\tau_r)$ represent the number of excited sites that are characterized by the radiative decay τ_r. The total luminescence intensity can be then expressed as follows:

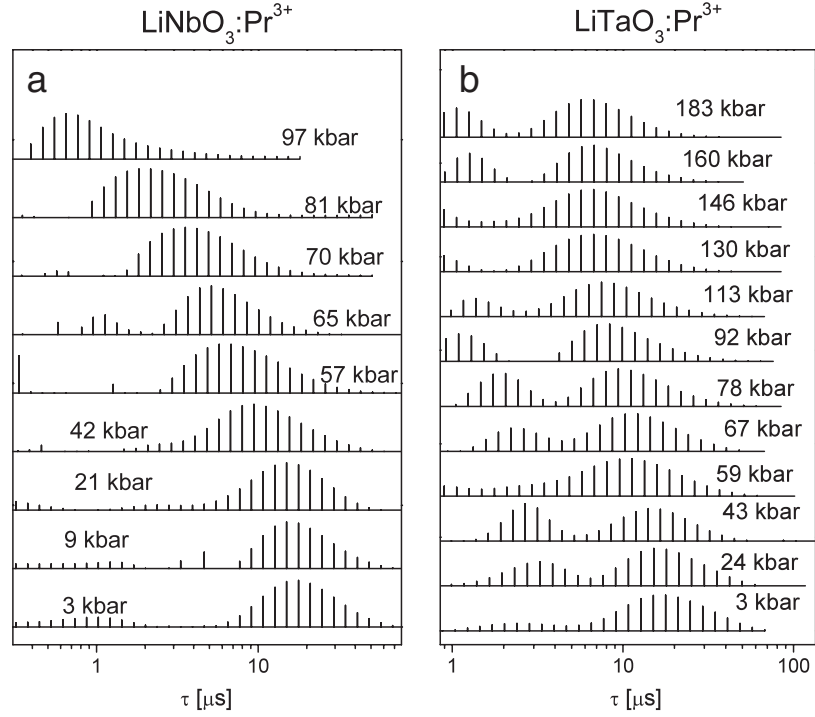$$I(t) = \int d\tau \frac{A(\tau)}{\tau} e^{-t/\tau} = \int d(\ln \tau) A(\tau) e^{-t/\tau}. \tag{4}$$
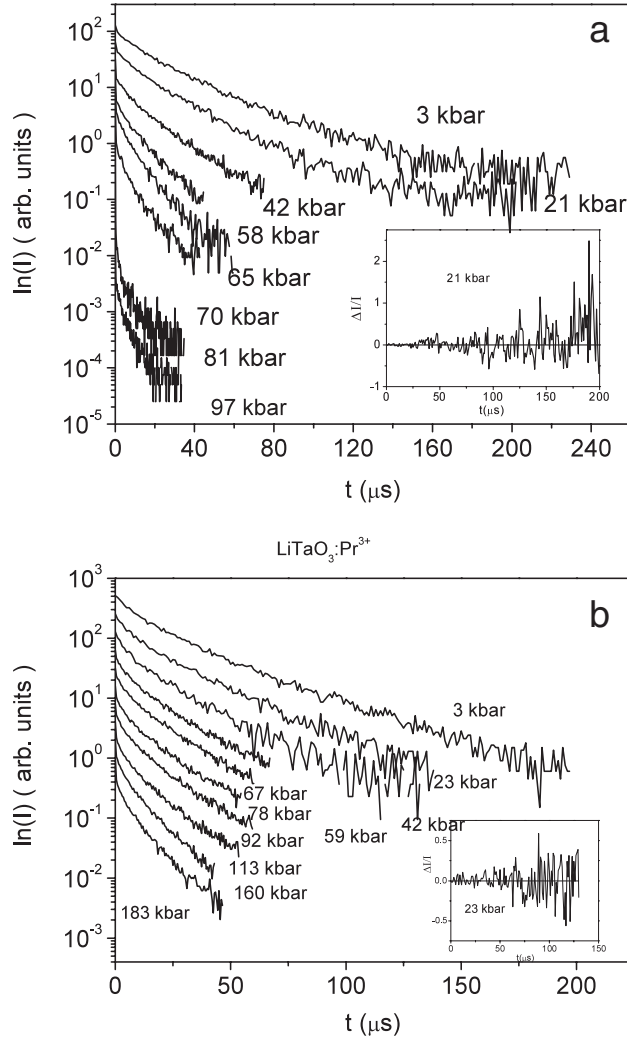
Figure 3. $^1D_2 \rightarrow ^3H_4$ luminescence decays for selected pressures for LiNbO$_3$:Pr^{3+} (a) and LiTaO$_3$:Pr^{3+} (b). In the insets of the figures the amount of relative dispersion of the fitted decay given by relation (8), obtained at 21 kbar and for 23 kbar for LiNbO$_3$:Pr^{3+} and LiTaO$_3$:Pr^{3+}, respectively, is presented.

In relation (4), $d\tau$ was replaced by $d(\ln \tau)$. This allows us to use the numerical procedure based on fitting to the experimental decays theoretical functions of the type

$$I(t) = \sum_i A_i(\tau_i)e^{-t/\tau_i} \tag{5}$$

where the finite but large-number lifetimes τ_i differ by a constant interval in the logarithmic scale. During fitting the lifetimes τ_i were kept constant and the fitting parameters were the quantities A_i that represent the recovered lifetime distribution function that can be presented in the form of a histogram.

We have used a nonlinear last square fit analysis [16] whereby χ^2 of the luminescence decay profile has been minimized. This function is defined as

Figure 4. The histograms representing the recovered lifetimes distribution of the $^1D_2 \rightarrow {}^3H_4$ luminescence for selected pressures for LiNbO$_3$:Pr^{3+} (a) and LiTaO$_3$:Pr^{3+} (b).

$$\chi^2 = \sum_k \left[\frac{I(t_k) - I_{\mathrm{ex}}(t_k)}{\sigma_k} \right]^2 \tag{6}$$

where $I(t_k)$ is the theoretical decay function given by relation (5), $I_{\mathrm{ex}}(t_k)$ is the experimental emission intensity and σ_k is the weighting of the experimental point, k. The weight constants were chosen to reflect the actual error associated with the individual experimental points. The weightings chosen are therefore

$$\sigma_k = \tfrac{1}{6} \sum_{l=-3}^{2} |I_{\mathrm{ex}}(t_{k-l}) - I_{\mathrm{ex}}(t_{k-l-1})|. \tag{7}$$

FORTRAN procedures, which minimize χ^2 using the Levenberg–Marquardt method [17], were used for the final solutions. 90–250 data points per decay curve of the original experiment data were used. The lifetime distribution was then approximated by 14 various lifetimes per decade. The quality of the fits can be seen when one plots the relative dispersion of the fitted decay given by following relation:

$$\frac{\Delta I}{I} = \frac{I_{\mathrm{ex}}(t) - I(t)}{I(t)}. \tag{8}$$

This quantity is plotted for selected cases and presented in the insets of figures 3(a) and (b).

The fitted lifetime distributions for different pressures are presented in the form of the histograms in figures 4(a) and (b) for LiNbO$_3$:Pr^{3+} and LiTaO$_3$:Pr^{3+}, respectively. It is seen that in both materials at ambient pressure the maxima of the lifetime distribution peaks at about 17 μs, which is in qualitative accordance with the results obtained earlier for LiNbO$_3$:Pr^{3+} [4]

and LiTaO$_3$:Pr^{3+} [8]. Then, with increasing pressure the lifetime distributions shift to shorter times. The shift is stronger for LiNbO$_3$:Pr^{3+}. Apart from the long-living emission, especially in the case of LiTaO$_3$, an additional maximum peaking at about 1–3 μs appears in the lifetime distribution function. This maximum also shifts to shorter lifetime with pressure.

To perform a quantitative analysis of the number of sites whose emission decays with respective lifetime one should remember that the area under the histograms, presented in figures 4(a) and (b), restricted by decays τ_1 and τ_2, does not represent the number of sites for which decay times are between τ_1 and τ_2. Relations (1) and (4) have been obtained under the assumption that the quantity $A(\tau) = \frac{dN(\tau)}{d\tau}$, and thus the number of sites decaying with times between τ_1 and τ_2 is given as

$$N(\tau_1, \tau_2) = \int_{\tau_1}^{\tau_2} A(\tau) \, d\tau = \int_{\ln(\tau_1)}^{\ln(\tau_2)} A(\tau) \cdot \tau \cdot d\ln(\tau). \tag{9}$$

Relation (9) yields that the number of sites that contribute to the emission with lifetime in the range $\ln \tau_1 < \ln \tau < \ln \tau_2$ is proportional to $A(\tau) \cdot \tau$. Thus the number of sites decaying with lifetimes of the order of a μs is much smaller (approximately ten times) than the number of sites that contribute to the emission with lifetimes of the order of tenths (seventeen) of a μs.

We consider that the emissions decaying with lifetimes of 3 and 17 μs in LiTaO$_3$:Pr^{3+} are related to two different Pr^{3+} sites. One notices that short-time emission is evidently observed only in LiTaO$_3$. In LiNbO$_3$ we probably only have Pr^{3+} sites that decay with longer lifetime. The multisite effect in LiTaO$_3$ and LiNbO$_3$ is related to the necessity of charge compensation of the triply charged praseodymium ion that replaces the Li$^+$ ion. One of the possibilities of such compensation results from the existence of Li$^+$ vacancies in non-stoichiometric crystals (we need two Li$^+$ vacancies to compensate the single Pr^{3+} in a Li$^+$ site). If one of such vacancies appears as the next neighbour of the Pr^{3+} ion, we have short distance compensation that creates quite a large odd-parity field that breaks the parity selection rule and significantly diminishes the emission lifetime. In stoichiometric crystals the majority of the Pr^{3+} ions are compensated by other defects (not necessarily point defects) and a small number of Li$^+$ vacancies are randomly distributed in the crystal (far from Pr^{3+}). So if compensation over a short distance takes place it is a very minor effect.

The problem of compensation of a triply ionized impurity by Li$^+$ vacancies has been discussed for LiTaO$_3$ doped with Cr^{3+} [18]. In our case both LiTaO$_3$ and LiNbO$_3$ have been grown from congruent melts in the same way but, in contrast to the LiNbO$_3$ crystal, it is very difficult to grow LiTaO$_3$ with the stoichiometric composition. As a result, we can assume that we have many more Li$^+$ vacancies in our LiTaO$_3$ than in LiNbO$_3$ and this is a reason why the short distance compensation is more probable in LiTaO$_3$:Pr^{3+} than in LiNbO$_3$:Pr^{3+}.

For quantitative analysis of the pressure dependence on the emission kinetics of the Pr^{3+} $^1D_2 \rightarrow {}^3H_4$ emission in LiNbO$_3$:Pr^{3+} and LiTaO$_3$:Pr^{3+} we have defined the effective emission lifetime as the lifetime corresponding to the maximum of the lifetime distribution. The respective data that represent the longer lifetimes are presented in figure 5.

Although the kinetics of the Pr^{3+} emission and effective emission lifetime at ambient pressure are almost the same for LiNbO$_3$:Pr^{3+} and LiTaO$_3$:Pr^{3+} their pressure evolution is quite different. Diminishing of the $^1D_2 \rightarrow {}^3H_4$ emission lifetime of the LiTbO$_3$:Pr^{3+} system is quite moderate; it stops at pressures above 120 kbar and is not accompanied by luminescence quenching [9]. In contrast, for the same emission in LiNbO$_3$:Pr^{3+} the lifetime diminishes linearly with pressure by more than an order of magnitude and this diminishing is accompanied by the luminescence quenching effect. As a consequence the emission related to the $^1D_2 \rightarrow {}^3H_4$ transition in LiNbO$_3$:Pr^3 disappears at pressures above 100 kbar at room temperature [13].
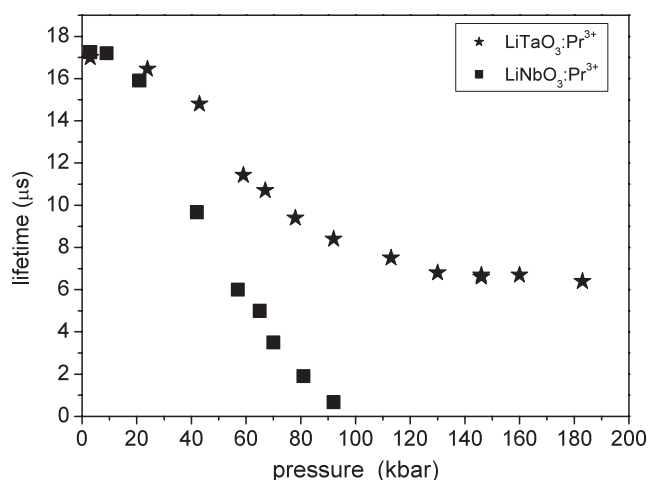
Figure 5. The effective lifetimes of $^1D_2 \rightarrow {}^3H_4$ LiNbO$_3$:Pr^{3+} (rectangles) and LiTaO$_3$:Pr^{3+} (asterisks) versus pressure.

Such different pressure behaviour of the emission lifetimes and efficiencies suggests that we are dealing with two different phenomena responsible for the observed effect.

It has been already shown that in LiNbO$_3$:Pr^{3+} [10, 13] an exciton trapped at the praseodymium ion contributes to the energetic structure of the centre by the states with the lowest energies above and not far from the energy of the $^1D_2$ state, but below or very close to the $^3P_0$ state. It has also been shown that the energy of the trapped exciton state diminishes with pressure, and that the effective intra-centre energy transfer from the $^1D_2$ excited state of Pr^{3+} to the trapped exciton state becomes effective for pressures above 100 kbar [13]. As a result, for higher pressures one observes the broad band luminescence seen in figure 2(a). This is a reason why the diminishing of the $^1D_2 \rightarrow {}^3H_4$ emission lifetime in LiNbO$_3$:Pr^3 could be related mainly to the non-radiative depopulation of the $^1D_2$ state through the Pr^{3+} trapped exciton state.

In contrast, the energies of the Pr^{3+} trapped exciton states in the LiTaO$_3$:Pr^{3+} are higher and the lowest state of this system is placed far above the energy of the $^3P_0$ state [9]. The diminishing of the trapped exciton energy with pressure causes the fact that in LiTaO$_3$:Pr^{3+} one observes damping of the $^3P_0 \rightarrow {}^3H_4$ luminescence with increasing pressure, whereas the intensity of the $^1D_2 \rightarrow {}^3H_4$ remains unchanged. Thus, the diminishing of the $^1D_2 \rightarrow {}^3H_4$ emission lifetime with pressure cannot be related to the influence of the trapped exciton. The effect in this case is related rather to the pressure-induced odd parity stress of the local Pr^{3+} ion coordination. An additional argument for such an interpretation is provided by the luminescence spectra. In figure 2(b) it is seen that pressure changes the relative intensities of the fine lines indicated as A and B, which represent two transitions from the lowest component of the $^1D_2$ state to components of the ground state split in the crystal field of C$_{3v}$ symmetry, $\Gamma_3(^1D_2) \rightarrow \Gamma_2\Gamma_3(^3H_4)$ and $\Gamma_3(^1D_2) \rightarrow \Gamma_1(^3H_4)$, respectively [9].

3. Conclusions

Photoluminescence kinetics related to the $^1D_2 \rightarrow {}^3H_4$ transition in Pr^{3+} ions in LiNbO$_3$:Pr^{3+} and LiTaO$_3$:Pr^{3+} crystals have been investigated at different pressures. We have noticed two different mechanisms that are responsible for diminishing of the luminescence lifetimes with pressure that are related to the actual energy of the Pr^{3+} trapped exciton states in these materials.

In $LiNbO_3$:Pr^{3+}, where at ambient pressure the energy of the trapped exciton is the same as or a little smaller than the energy of the $^3P_0$ but higher than energy of the $^1D_2$ state, the diminishing of the lifetime is accompanied by damping of the $^1D_2 \rightarrow ^3H_4$ luminescence. Therefore we have considered that the main reason for the lifetime diminishing is related to the non-radiative transfer of the excitation from the $^1D_2$ excited state of Pr^{3+} to the exciton trapped to the Pr^{3+}. The negative pressure shift of the energy of trapped exciton states causes the increase of both effects (lifetime decreasing and luminescence damping) with pressure.

In $LiTaO_3$, where the energy of the Pr^{3+} trapped exciton is larger than the energy of the $^3P_0$ state, in all the considered pressure range, the non-radiative energy transfer from the $^1D_2$ excited state to the exciton state is negligible. The small changes of the $^1D_2 \rightarrow ^3H_4$ luminescence lifetime are tentatively attributed to changes in the local environment of the Pr^{3+} ions induced by hydrostatic pressure.

Acknowledgments

References

[1] Miller R C and Nordland W A 1970 *Phys. Rev.* B **2** 4896
[2] Tangonan G L, Barnoski M K, Lotspeich J F and Lee A 1977 *Appl. Phys. Lett.* **30** 238
[3] Malinowski M, Joubert M-F and Jaqiuer B 1993 *Phys. Status Solidi* **140** k49
[4] Lorenzo A, Bausá L E and García Solé J 1995 *Phys. Rev.* B **51** 16643
[5] Lorenzo A, Jaffrezic H, Roux B, Boulon G, Bausá L E and García Solé J 1995 *Phys. Rev.* B **52** 6278
[6] Muñoz–Santiuste J E, Lorenzo A, Bausá L E and García Solé J 1998 *J. Phys.: Condens. Matter* **10** 7653
[7] Piramidowicz R, Pracka I, Woliński W and Malinowski M 2000 *J. Phys.: Condens. Matter* **12** 709
[8] Sokólska I, Ryba-Romanowski W, Gołąb S, Łukasiewicz T and Świrkowicz M 1997 *J. Phys.: Condens. Matter* **9** 5217
[9] Gryk W, Dyl D, Ryba-Romanowski W and Grinberg M 2005 *J. Phys.: Condens. Matter* **17** 5381
[10] Gryk W, Kukliński B, Grinberg M and Malinowski M 2004 *J. Alloys Compounds* **380** 230
[11] Lorenzo A, Jaffrezic H, Roux B, Boulon G and García Solé J 1995 *Appl. Phys. Lett.* **67** 3735
[12] Lorenzo A, Loro H, Muñoz-Santiuste J E, Terrile M C, Boulon G, Bausá L and García Solé J 1997 *Opt. Mater.* **8** 55
[13] Gryk W, Dyl D, Grinberg M and Malinowski M 2005 *Phys. Status Solidi* c **2** 188
[14] Pracka I, Malinowski M, Bajor A, Surma B, Gałązka Z, Świrkowicz M and Mozdzonek M 1997 *Proc. SPIE* **3178** 295
[15] Ryba-Romanowski W, Sokolska I, Golab S and Łukasiewicz T 1997 *Appl. Phys. Lett.* **70** 686
[16] Demas J N 1983 *Excited State Lifetime Measurements* (New York: Academic)
[17] Press W H, Flannery B P, Tenkolsky S A and Vetterling W T 1986 *Numerical Recipes, The Art of Scientific Computing* (Cambridge: Cambridge University Press)
[18] Grinberg M, Barzowska J, Shen Y R and Bray K L 2001 *Phys. Rev.* B **63** 214104